IF UC-95-25

STATE RESEARCH CENTER OF RUSSIA

INSTITUTE FOR HIGH ENERGY PHYSICS

FERMILAB
FEB 1 1996
LIBRARY

IHEP 95-25

L.G. Landsberg, V.V. Molchanov

Fermilab Library
0 1160 0050536 4

ON THE SEARCH FOR CRYPTOEXOTIC STRANGE BARYONS WITH ADDITIONAL HIDDEN STRANGENESS IN THE EXPERIMENTS WITH HIGH ENERGY HYPERON BEAMS

31

Zielinski 2669 359

Protvino 1995

UDK 681.3.06.069 M–24

Abstract

Landsberg L.G., Molchanov V.V. On the Search for Cryptoexotic Strange Baryons with Additional Hidden Strangeness in the Experiments with High Energy Hyperon Beams.: IHEP Preprint 95-25. – Protvino, 1995. – p. 31, figs. 17, tables 2, refs.: 32.

Data on possible existence of cryptoexotic baryons with hidden strangeness are considered. Possible searches for strange exotic baryons with additional hidden strangeness in the Σ^--beam in the experiment E781 are discussed.

Аннотация

Ландсберг Л.Г., Молчанов В.В. О возможных поисках криптоэкзотических странных барионов с дополнительной скрытой странностью в экспериментах на гиперонных пучках высоких энергий: Препринт ИФВЭ 95-25. – Протвино, 1995. – 31 с., 17 рис., 2 табл., библиогр.: 32.

Рассмотрены данные о возможном существовании экзотических барионов со скрытой странностью. Обсуждаются поиски странных экзотических барионов с дополнительной скрытой странностью в Σ^--пучке в эксперименте E781.

© State Research Center of Russia
Institute for High Energy Physics, 1995

1. Introduction

The rapid development of hadron spectroscopy in recent years has led to significant advance in the systematics of "ordinary" hadrons with the simplest valence quark structure: $q\bar{q}$ for mesons and qqq for baryons. At the same time several unusual hadrons with some anomalous features have been found. They do not fit into this simplest quark model systematics and are interpreted as new forms of hadronic matter — exotic hadrons. These states can include multiquark formations ($qq\bar{q}\bar{q}$ mesons and $qqqq\bar{q}$ baryons), hybrid systems with valence quarks and gluons ($q\bar{q}g$ mesons and $qqqg$ baryons), or glueballs, i.e. mesons consisting solely of valence gluons (gg, ggg). The discovery of the exotic hadrons would have far-reaching consequences for quantum chromodinamics, for the concept of confinement and specific models of hadron structure (lattice, string and bag models).

Detailed discussions of exotic hadron physics can be found in recent reviews [1–5].

Exotic hadrons can have anomalous quantum numbers not accessible to three-quark baryons or quark-antiquark mesons (open exotic states) or even usual quantum numbers (cryptoexotic states). Cryptoexotic hadrons can be identified only by their unusual dynamical properties (anomalously narrow decay widths, anomalous decay branching ratios and so on).

As it is clear from review papers [1–5], in the last decade searches for exotic mesons have led to considerable advance in this field. Several new states have been observed whose properties cannot be explained by using the naive quark model of ordinary mesons with $q\bar{q}$ valence quark structure. These states are serious candidates for exotic mesons (most of them are of cryptoexotic type).

At the same time the situation for exotic baryons is far from being clear. There were also some examples of possible unusual baryon resonances [6–9], but these data are not quite accurate and are not supported by some new experimental results [5, 10–12].

The recent data of the SPHINX experiment at IHEP 70 GeV accelerator [13–17] gave new important evidence of possible existence of cryptoexotic baryons with hidden strangeness ($uuds\bar{s}$ valence quark structure) $X(2050)^+ \to \Sigma(1385)^0 K^+$ and $X(2000) \to \Sigma^0 K^+$. We shall briefly summarize these data in Sect. 4, after a general description of

nature and expected properties of cryptoexotic baryons as well as several promising ways for their production and observation.

But the main part of this paper is connected with the proposal of future measurements with the hyperon beam of high energy at the Fermilab Tevatron (experiment E781) to search for possible strange exotic baryons with additional hidden strangeness $Y_\phi = \mid ddss\bar{s}\rangle$ in the diffractional reactions in $\Sigma^- N$ and Σ^-(nucleus) interactions.

2. Cryptoexotic baryons

As it was stated before, cryptoexotic baryons do not have external exotic features and their complex internal valence structure can be established indirectly by examining their anomalous dynamical properties (such as small decay widths, unusual decay branching ratios and so on).

The searches for heavy baryons with anomalously narrow decay widths, would they be successful, make it possible to obtain the best evidence of cryptoexotic baryon states. In this connection let us consider the properties of multiquark baryons with hidden strangeness $B_\phi = \mid qqqs\bar{s}\rangle$ $(q = u, d, s)$.

If such cryptoexotic baryon structure consists of two color parts separated in space because of a centrifugal barrier, then its decays into the color singlet final states may be suppressed because of complicated quark rearrangement in these processes. The properties of multiquark exotic baryons with internal color structure

$$\mid qqqq\bar{q}\rangle_{1c} = \mid (qqq)_{8c} \odot (q\bar{q})_{8c}\rangle \tag{1}$$

(color octet bonds) or

$$\mid qqqq\bar{q}\rangle_{1c} = \mid (qq\bar{q})_{\bar{6}c} \odot (qq)_{6c}\rangle \tag{2}$$

(color sextet-antisextet bonds) are discussed in [18–20]. Here subscripts 1c, 8c and so on specify the representation of the color $SU(3)_c$ group. If the mass of nonstrange baryon with hidden strangeness is above the threshold for the decay modes with the strange particles in final states then the main decay channels should be of the type

$$B_\phi \to YK + n\pi \tag{3}$$

or

$$B_\phi \to \phi N(\eta N; \eta' N) + n\pi \tag{4}$$

(n = 0, 1, ...), i.e. with strange particle pairs or with particles with significant hidden strangeness component in their valence quark structure. The nonstrange decays of baryons with hidden strangeness $B_\phi \to N + n\pi$ must be suppressed because of the continuous quark line rule ("OZI suppression").

For the strange baryons with hidden strangeness the main decay channels must be with multiple strange particle production in the final states, i.e. $Y_\phi \to \Sigma K\overline{K}(\Lambda K\overline{K}) + n\pi$ or $Y_\phi \to \Xi\overline{K} + n\pi$.

Depending on the mechanism of quark rearrangement in the decay processes the widths of the massive cryptoexotic baryons may be significantly reduced and, in principle, can be anomalously narrow (of the order of several tens of MeV). The theoretical predictions here are quite arbitrary [18–21]. So the question of the existence of such narrow baryon resonances with hidden strangeness can be resolved only with experiments and it seems quite desirable to perform the search for cryptoexotic baryons with anomalous dynamical features which are different from the properties of usual (qqq)-isobars [22]. These anomalous features are:

1. The main decay modes of these baryons are with additional strange pairs in the final states (for usual baryons such decays have branching ratios at the percent level).
2. Heavy enough baryonic mass ($M > 2\,\mathrm{GeV}$) with narrow enough decay width because of quark rearrangement and limited phase space for OZI allowed decays ($\Gamma \leq 50 \div 100\,\mathrm{MeV}$).

3. Diffractive production processes and reactions with multiple Pomeron rescattering

As it is stated in a number of papers [2, 5, 6, 10, 19], the diffractive production reactions with Pomeron exchange offer some new possibilities to search for exotic hadrons especially in the high energy region, since the cross sections of these exclusive processes do not decrease with energy. According to modern notions, Pomeron is a multigluon system, which leads to a possibility of exotic hadron production in diffractional processes (see the diagrams on Fig. 1). Indeed, as it is apparent from the Pomeron exchange mechanism for the diffractive reactions, only the states with the same charges and flavors as for the primary hadron can be produced in these processes. Besides, there is an additional limitation for the quantum numbers of the hadrons to be produced, which is stipulated by the Gribov-Morrison selection rule for changing the parity (ΔP) and spin (ΔJ) in the transitions from a primary hadron to a diffractively produced hadronic system: $\Delta P = (-1)^{\Delta J}$. For example, in the proton diffraction only baryonic states with natural sets of quantum numbers $J^P = 1/2^+; 3/2^-; 5/2^+; 7/2^-$ etc. can be excited due to this rule. But the Gribov-Morrison selection rule is not a rigorous law and is of an approximate character.

In spite of all these limitations and serious problems with the separation between the diffractive production of resonance states and some nonresonance hadron clusters it should be noted that the diffractive production mechanism seems to be quite perspective in searching and observation of new exotic hadrons. It is also possible to search for the states with new flavors in the processes of diffractive pair production [23].

The Pomeron exchange mechanism in diffractive production reactions opens a possibility to study coherent processes on the target nuclei. It has been suggested that coherent production on nuclei is a good tool for the separation of resonances against the multiparticle background because of the difference in their absorption in the target nuclei [24].

The use of coherent reactions on nuclei, i.e. processes with very small P_T^2 is not the only way for the better separation of resonance production against the background. In some cases the best conditions for the exotic hadron searches can be obtained in the region of big enough or intermediate transverse momenta ($P_T^2 \geq 0.2 \div 0.3\,\mathrm{GeV}^2$), where the background from peripheral processes is strongly reduced. It should be noted that the exotic hadron production in the intermediate P_T^2 region could take place through the multiple Pomeron exchange mechanism (i.e. again through multigluon process). For example, in the study of the charge-exchange reactions $\pi^- p \to \eta\eta + \Delta^0$ and $\pi^- p \to \eta\eta' + n$ after the selection of events with $P_T^2 \geq 0.2 \div 0.3\,\mathrm{GeV}^2$ unusually narrow meson states $X(1740) \to \eta\eta$ [25, 26] and $X(1910) \to \eta\eta'$ [27, 28] were observed. These anomalous states are good candidates for cryptoexotic mesons. The mechanism of multiple rescattering with Pomeron exchange may explain the $X(1740)$ and $X(1910)$ production (Fig. 2a) [29].

For the case of very high energy instead of charge exchange reactions of Fig. 2a type, the diffractive production with rescattering (Fig. 2b) can be used for the nonperipheral exotic hadron searches. The cross sections for these processes must be energy independent. The use of $P_T^2 > 0.2 \div 0.3\,\mathrm{GeV}^2$ cut in the diffractive production gives the possibility to separate these gluon-rich rescattering processes with multipomeron exchange and to search for new exotic hadrons in this region.

4. Study of the diffractive reactions $p + N \to Y^* K + N$ with the SPHINX spectrometer and search for cryptoexotic nonstarnge pentaquark baryons with hidden strangeness

In the experiments of the SPHINX Collaboration a wide program of studying the hadron diffractive production by protons with $E_p = 70\,\mathrm{GeV}$ and the search for cryptoexotic baryons in these processes were carried out in the proton beam of the IHEP accelerator. This program has been detailed in [2, 5, 10–17]. The most important results of these measurements were obtained in the study of the diffractive coherent reactions on carbon nuclei

$$p + \mathrm{C} \;\to\; [\Sigma(1385)^0 K^+] + \mathrm{C}, \qquad (5)$$
$$\hookrightarrow \Lambda\pi^0$$

and

$$p + \mathrm{C} \;\to\; [\Sigma^0 K^+] + \mathrm{C}. \qquad (6)$$
$$\hookrightarrow \Lambda\gamma$$

The SPHINX facility [10], which is used for these measurements, includes a wide-aperture magnetic spectrometer with scintillation counter hodoscopes, proportional chambers, drift chambers and multichannel γ-spectrometer with lead glass total absorbtion detectors. The charged particles in the final state were identified by means of a RICH differential Cherenkov spectrometer and two threshold gas multicell Cherenkov counters.

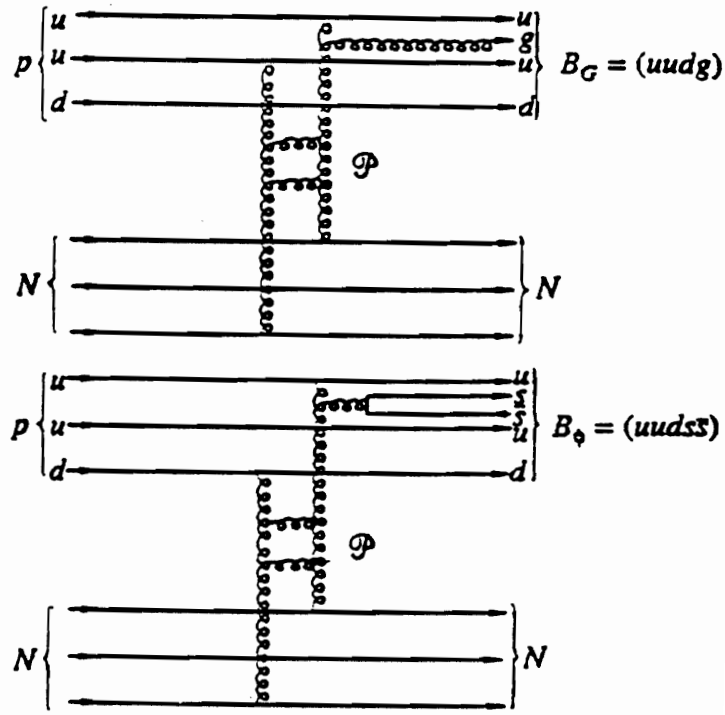

Fig. 1. The diagrams for the exotic baryon production in diffractional processes with the Pomeron exchange.

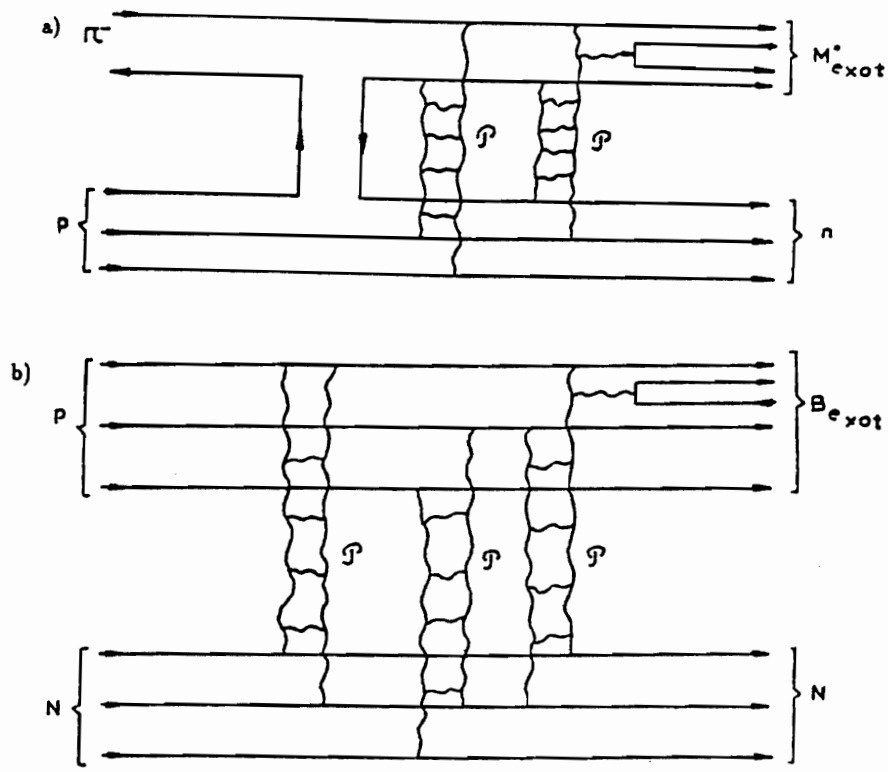

Fig. 2. The diagrams for the exotic hadron production with the machanism of the multiple Pomeron exchange: a) in charge-exchange reactions; b) in diffractive production reactions.

4.1. Reaction $p + N \to \Sigma(1385)^0 K^+ + N$

In the analysis of the SPHINX data the exclusive process with Λ-hyperons $p + N \to [\Lambda\pi^0 K^+] + N$ was identified [12, 13]. In Fig. 3 the effective mass spectrum of the $\Lambda\pi^0$ system in this reaction is presented. In $M(\Lambda\pi^0)$ mass spectrum the peak of $\Sigma(1385)^0 \to \Lambda\pi^0$ is dominating. The background level under the $\Sigma(1385)^0$ peak is quite small. This fact simplifies the identification of reaction (5).

Coherent events of reaction (5) were singled out in the analysis of $\mathrm{d}N/\mathrm{d}P_T^2$ distribution as a strong forward peak with the slope $b > 30\,\mathrm{GeV}^{-2}$. In order to reduce the noncoherent background and obtain the $\Sigma(1385)^0 K^+$ mass spectrum for "pure" coherent production reaction on carbon nuclei a stringent requirement $P_T^2 < 0.02\,\mathrm{GeV}^2$ has been used and the mass spectra of $\Sigma(1385)^0 K^+$ for the coherent events of (5) has been obtained (see, for example, Fig. 4). These spectra were studied with different values of ΔM bin widths in histograms and with bin shifting. The thorough background evaluation under the peaks was obtained using the information on the side bands near the peak. The statistical confidence levels of the peaks were determined from these data.

The fits of the spectra with Breit-Wigner peaks and polynomial smooth background were carried out, and the average values for the main parameters of $X(2050)$ structure were determined:

$$\left.\begin{array}{l} M = 2052 \pm 6\,\mathrm{MeV}; \\ \Gamma = \left(35^{+22}_{-35}\right)\mathrm{MeV} \\ \text{(with the account of the apparatus mass resolution);} \\ \text{statistical C.L. of the peak} > 5 \div 8 \text{ s.d.} \end{array}\right\} \tag{7}$$

This narrow structure cannot be explained by diffractive nonresonant process of the Deck-type and seems to be caused by the production of a new cryptoexotic baryon with hidden strangeness.

4.2. Reaction $p + N \to [\Sigma^0 K^+] + N$

During the study of the reaction with Λ-hyperons and K-mesons the events with one and only one additional γ-cluster detected in γ-spectrometer of the SPHINX apparatus were separated.

The effective mass spectrum of $\Lambda\gamma$ system for these events is shown in Fig. 5. The peak of $\Sigma^0 \to \Lambda\gamma$ decay in this spectrum is clearly seen. Thus, reaction (6) is identified and coherent events are singled out using P_T^2 distribution.

The effective mass spectrum $M(\Sigma^0 K^+)$ for coherent reaction (6) with $P_T^2 < 0.1\,\mathrm{GeV}^2$ is presented in Fig. 6. In this spectrum besides of some small structure with $M \sim 1800\,\mathrm{GeV}$ in the threshold region, a strong peak $X(2000)$ is clearly observed. The main parameters of $X(2000)$ structure are:

$$\left.\begin{array}{l} M = 1997 \pm 7\,\mathrm{MeV}; \\ \Gamma = 91 \pm 17\,\mathrm{MeV}; \\ \text{statistical C.L. of the peak} > 7 \text{ s.d.} \end{array}\right\} \tag{8}$$

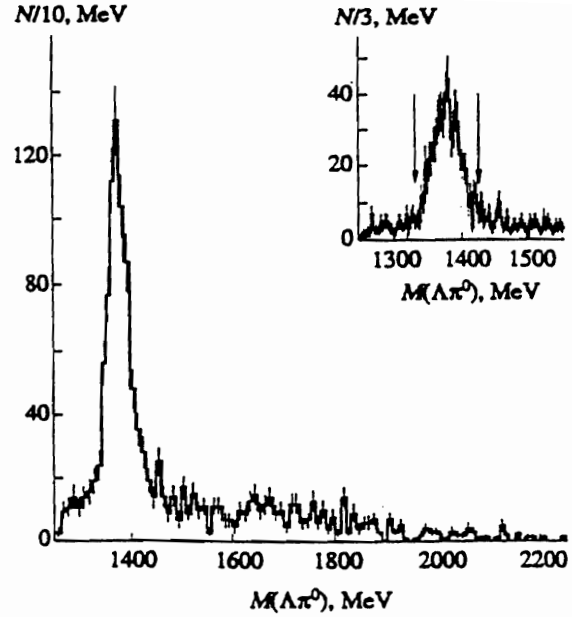

Fig. 3. The invariant mass spectrum of $\Lambda\pi^0$ system in reaction $p + N \to [\Lambda\pi^0 K^+] + N$. The parameters of $\Sigma(1385)^0$ peak are $M = 1377 \pm 3\,\mathrm{MeV}$ and $\Gamma = 39 \pm 3\,\mathrm{MeV}$. They are in agreement with the tabulated values of these parameters (with the account of apparatus mass resolution $\sigma = \pm 9\,\mathrm{MeV}$ and systematic errors). The arrows indicate the region of $\Sigma(1385)^0$ band.

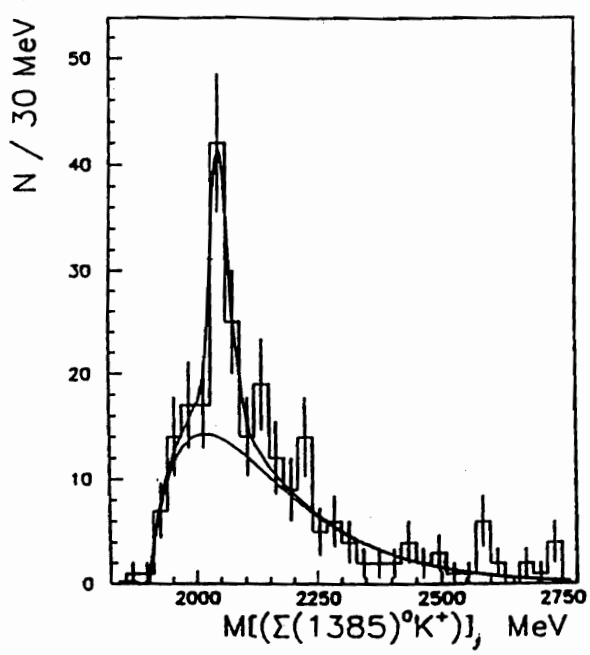

Fig. 4. The effective mass spectrum $M[\Sigma(1385)^0 K^+]$ in coherent reaction on carbon nucleus $p + C \to \Sigma(1385)^0 K^+ + C$ at $P_T^2 < 0.02\,\mathrm{GeV}^2$. The spectrum is fitted by the sum of the smooth polynomial background and the Breit-Wigner peak with parameters: $M = 2035 \pm 5\,\mathrm{MeV}$ and $\Gamma = 35 \pm 16\,\mathrm{MeV}$.

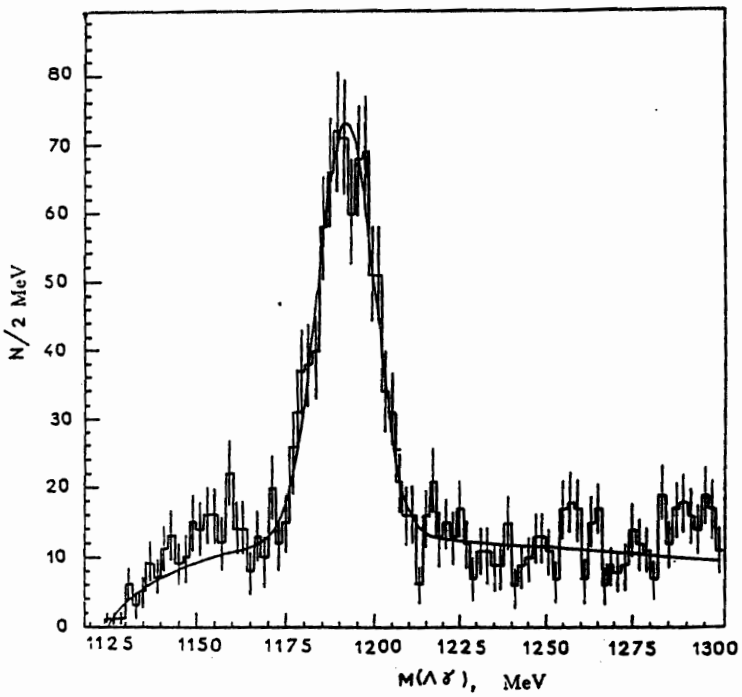

Fig. 5. The effective mass spectrum $\Lambda\gamma$ in the reaction $p + N \rightarrow [\Lambda\gamma K^+] + N$. The peak of Σ^0 hyperon is clearly seen in this spectrum.

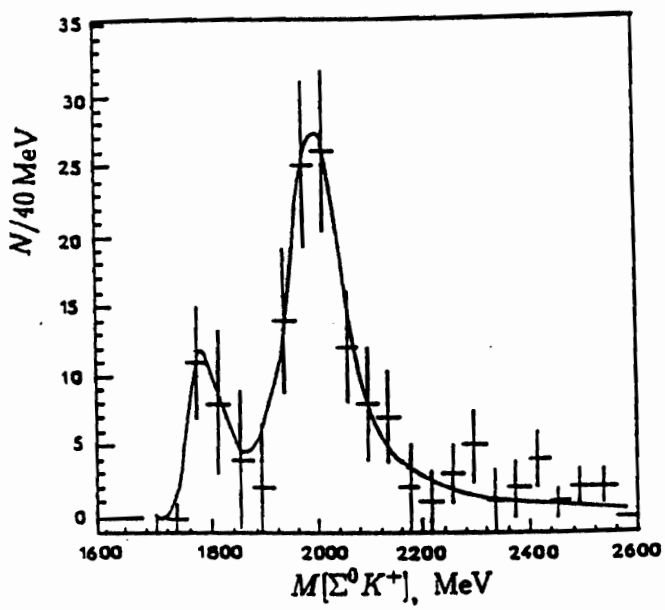

Fig. 6. The effective mass spectrum $M(\Sigma^0 K^+)$ for the coherent diffractive reaction $p + C \rightarrow [\Sigma^0 K^+] + C$ at $P_T^2 < 0.1\,\mathrm{GeV}^2$. In this spectrum some structure in the threshold region with $M = 1802 \pm 3\,\mathrm{MeV}$ and a clear peak with $M = 1999 \pm 7\,\mathrm{MeV}$ and $\Gamma = 91 \pm 17\,\mathrm{MeV}$ are observed.

Such shape of mass spectrum $\Sigma^0 K^+$ (with additional structure in the threshold region) shows that $X(2000)$ peak cannot be explained by nonresonant Deck-type diffractive singularity. It seems that this peak has a resonant nature.

4.3. Study of other decay channels for $X(2050)$ and $X(2000)$ states

To search for other decay channels for $X(2050)$ and $X(2000)$ baryon states the simultaneous analysis of the SPHINX data on the coherent reactions

$$p + \mathrm{C} \rightarrow p\pi^+\pi^- + \mathrm{C} \tag{9}$$

$$\rightarrow \Delta(1232)^{++}\pi^- + \mathrm{C} \tag{10}$$

has been performed together with (5) and (6) and under the same kinematical conditions. Preliminary data on the reaction of $[\Delta(1232)^{++}\pi^-]$ production were obtained in our previous work [13]. The diffractive production of some isobar-like structures with mass $\approx 1460\,\mathrm{MeV}$ and $\approx 1715\,\mathrm{MeV}$ were clearly seen in these data.

But in the mass region of $X(2050)$ and $X(2000)$ states there are no such structures in all mass spectra of $M(p\pi^+\pi^-)$ and $M[\Delta(1232)^{++}\pi^-]$ in reactions (9) and (10). The lower limits for the ratios of the corresponding decay branchings were estimated to be (with 95% C.L.):

$$\mathrm{R}_1 = \frac{\mathrm{BR}\{X(2050)^+ \rightarrow [\Sigma(1385)K]^+\}}{\mathrm{BR}\{X(2050)^+ \rightarrow [\Delta(1232)\pi]^+\}} > 1.7\,, \tag{11}$$

$$\mathrm{R}_2 = \frac{\mathrm{BR}\{X(2050)^+ \rightarrow [\Sigma(1385)K]^+\}}{\mathrm{BR}\{X(2050)^+ \rightarrow p\pi^+\pi^-\}} > 2.6\,, \tag{12}$$

$$\mathrm{R}_2' = \frac{\mathrm{BR}\{X(2050)^+ \rightarrow \Sigma(1385)^0 K^+\}}{\mathrm{BR}\{X(2050)^+ \rightarrow p\pi^+\pi^-\}} > 0.86\,, \tag{13}$$

$$\mathrm{R}_3 = \frac{\mathrm{BR}\{X(2000)^+ \rightarrow [\Sigma K]^+\}}{\mathrm{BR}\{X(2000)^+ \rightarrow [\Delta(1232)\pi]^+\}} > 0.83\,, \tag{14}$$

$$\mathrm{R}_4 = \frac{\mathrm{BR}\{X(2000)^+ \rightarrow [\Sigma K]^+\}}{\mathrm{BR}\{X(2000)^+ \rightarrow p\pi^+\pi^-\}} > 7.8\,, \tag{15}$$

$$\mathrm{R}_4' = \frac{\mathrm{BR}\{X(2000)^+ \rightarrow \Sigma^0 K^+\}}{\mathrm{BR}\{X(2000)^+ \rightarrow p\pi^+\pi^-\}} > 2.6\,. \tag{16}$$

Here the isotopic conditions for the decays of $X(2050)$ and $X(2000)$ baryons with isotopic spin $I = \frac{1}{2}$ were used (these states belong to isodoublets because they are produced in the diffractive dissociation of protons).

The ratios R_1–R_4 for $X(2050)$ and $X(2000)$ decays on strange and nonstrange particles are much larger than the same ratios for the decays of usual (qqq)-isobars (where they are of the order of several percent [22]).

The small enough widths of $X(2000)$ and $X(2050)$ baryon states as well as the anomalously large branching ratios for their decay channels with strange particles (large values of R_1–R_4) are the reasons to consider these states as serious candidates for the cryptoexotic baryons with hidden strangeness $\mid uuds\bar{s}\rangle$.

4.4. Conclusion from the SPHINX experiment

In the study of coherent diffractive production reactions (5) and (6) for the energy of proton beam $E_p = 70\,\mathrm{GeV}$ two new baryon structures $X(2050)^+ \rightarrow \Sigma(1385)^0 K^+$ and

$X(2000)^+ \to \Sigma^0 K^+$ were observed with statistically significant confidence level. These baryons are characterized by unusual dynamical features: small enough decay widths and anomalously high decay rates with strange particles in final states. Thus $X(2050)$ and $X(2000)$ are serious candidates for cryptoexotic baryons with hidden strangeness.

Certainly on the existing level of statistics the above results are considered as preliminary [17]. They should be confirmed in further measurements with greatly increased statistics. We hope to obtain by an order of magnitude larger amount of events of the processes (5) and (6) in a near future on the upgraded SPHINX setup.

The study of nonperipheral processes in reactions $p + N \to [\Sigma(1385)^0 K^+] + N$ and $p + N \to [\Sigma^0 K^+] + N$ in the region of intermediate transvers momenta $P_T^2 > 0.3$ GeV^2 was also performed in the SPHINX measurements. Some interesting effects in this region might be observed but the existing statistics is not enough to obtain any definite conclusion on this subject.

5. Experiment E781 at Fermilab (the SELEX Facility)

Possible evidence of narrow enough cryptoexotic baryon resonances of $B_\phi = \mid uuds\bar{s}\rangle$ type in the proton induced diffractive production reactions at the SPHINX spectrometer makes it quite desirable to continue the study of these pentaquark state candidates. In particular, it is important to search for strange cryptoexotic baryons with additional hidden strangeness $Y_\phi = \mid ddss\bar{s}\rangle$ in the diffractive production processes in the high energy Σ^--hyperon beam.

A wide research program in hyperon physics could be carried out in the experiment E781 at Fermilab with the SELEX facility in the hyperon beam of the Tevatron machine with the energy $E_{\Sigma^-} \simeq 600 \div 650$ GeV [30] by a large international collaboration.

The main part of this research program is connected with a high statistics study of the spectroscopy of charmed and strange-charmed baryons as well as weak decays of these states. It is expected to obtain several tens of thousands of events in each of the main decay channels of Λ_c, Ξ_c and Ω_c baryons. The high energy hyperon beam of Fermilab with high intensity opens some new possibilities for the search and study of exotic hadrons with strange and charmed quarks in different processes. Besides, it is planned to study some coherent production processes in the Coulomb field of heavy nuclei and in the diffractive reactions [23, 31].

The general layout of the SELEX facility is presented on Fig. 7. The apparatus is a three stage wide aperture magnetic spectrometer with proportional and drift chambers, vertex microstrip detector, trigger hodoscopes, additional microstrip detectors, 4 photon spectrometers, RICH and TRD detectors for particle identification, neutron calorimeter.

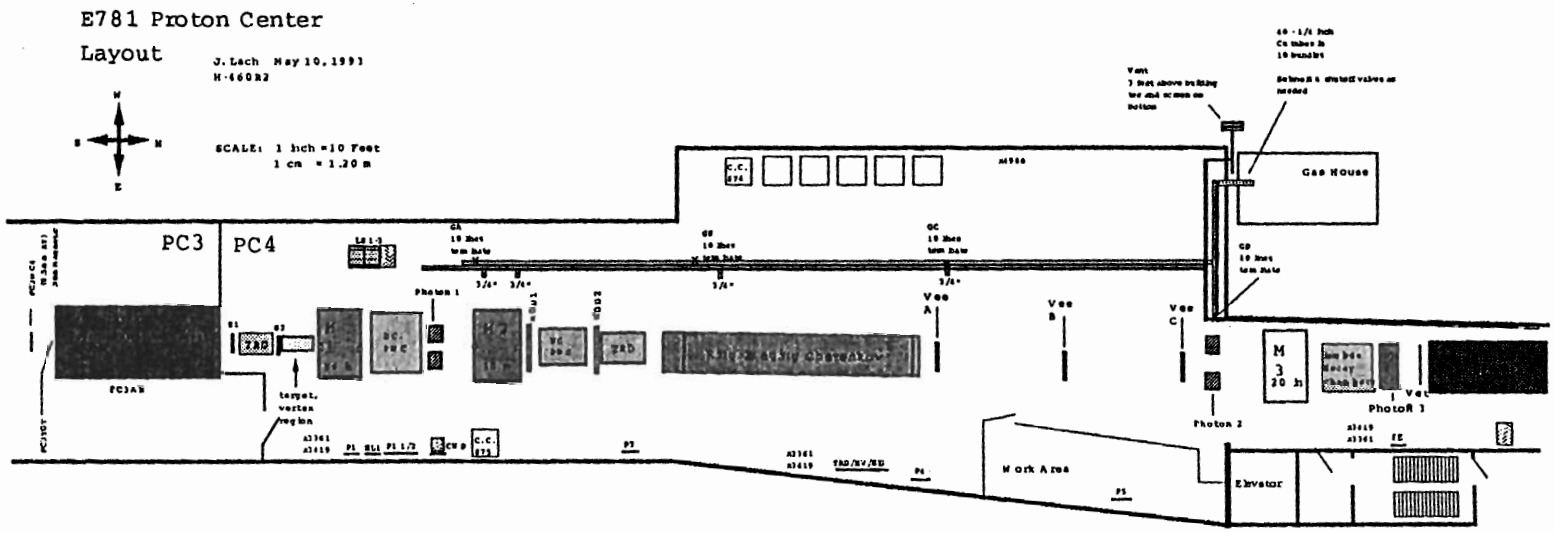

Fig. 7. The layout of the SELEX facility.

The main elements of the SELEX facility are as follows:

1. Detectors of the primary beam particle (scintillation counters S1 and S2, beam silicon strip detectors BSSD $X1$, $Y1$, $U1$, $X2$, $Y2$, $X3$, $Y3$, $U3$, beam TRD for pion-hyperon separation).
2. Targets (W, Ag, Cu, Si, C with total thickness corresponding to $\sim 5\%$ interactions of the beam particles) and two scintillation counters INTC to select the interactions in the target.
3. Vertex silicon strip detector VSSD $X1$, $Y1$, $U1$, $V1$, $X2$, $Y2$, $U2$, $V2$, $X3$, $Y3$, $U3$, $V3$, $X4$, $Y4$, $U4$, $V4$, $X5$, $Y5$, $U5$, $V5$, $X6$ (with dimensions from $51 \times 51\,\mathrm{mm}^2$ up to $90 \times 128\,\mathrm{mm}^2$).
4. Magnetic spectrometer M1 ($60.96 \times 50.8 \times 183\,\mathrm{cm}^3$) for slow particles.
5. Magnetic spectrometer M2 ($60.96 \times 25.4 \times 183\mathrm{cm}^3$) for fast particles.
6. Additional silicon strip detectors:
   a) TRSD1, TRSD2 ($10 \times 10\,\mathrm{cm}^2$) for 3 level trigger;
   b) LASD $X1$, $Y1$, $U1$, $X2$, $Y2$, $U2$ ($5.12 \times 5.12\,\mathrm{cm}^2$) in the magnetic field of M1 and $X3$, $Y3$, $U3$, $X4$, $Y4$, $U4$ ($8.96 \times 9.00\,\mathrm{cm}^2$) before M2; DSSD $X1$, $Y1$, $X2$, $Y2$, $U2$ ($8.96 \times 9.00\,\mathrm{cm}^2$) after M2.
7. The system of proportional and drift chambers:
   a) between M1 and M2 ($PX1$, $PY1$, $PU1$, $PV1$, $PX2$, $PY1$, $PX2$, $PY2$, $PU2$, $PV2$, $PX3$, $PY3$, $PU3$, $PV3$ with size $200 \times 200\,\mathrm{cm}^2$ and DC $X1$, $X2$, $X3$, $X4$ with size $200 \times 150\,\mathrm{cm}^2$);
   b) after M2: DPWC $X1$, $U1$, $V1$, $Y1$, $X2$, $Y2$ ($60 \times 60\,\mathrm{cm}^2$); $X3$, $Y3$, $U2$, $V2$, $X4$, $Y4$, $X5$, $Y5$ ($60 \times 100\,\mathrm{cm}^2$); DDCH $X1$, $X2$, $X3$, $X4$ ($100 \times 120\,\mathrm{cm}^2$).
8. Magnetic spectrometer for Λ-decay registration: magnet M3 ($60.96 \times 50.8 \times 182.8\,\mathrm{cm}^3$) with 3 clusters of drift chambers VEEA, VEEB, VEEC before M3 ($120 \times 120\,\mathrm{cm}^2$ with $X1$, $Y1$, $U1$, $X2$, $Y2$ planes in each drift chamber) and proportional chambers LPWC $V1$, $Y1$, $X1$, $U1$, $X2$, $Y2$, ($64 \times 64\,\mathrm{cm}^2$), $V2$ ($141 \times 141\,\mathrm{cm}^2$).
9. RICH detector with phototube matrix (2848 channels).
10. TRD detector for secondary particles.
11.

Four lead glass electromagnetic calorimeters:	Photon 1 (630 channels)	$15 \div 30 < \theta_\gamma < 100$ mrad
	Photon 2 (656 channels)	$7 < \theta_\gamma < 15 \div 30$ mrad
	Photon 3 (320 channels)	$\theta_\gamma < 8$ mrad
	Photon 4 (320 channels)	$\theta_\gamma < 8$ mrad

12. Neutron calorimeter NCAL.
13. Microstrip hodoscopes and fast hardware processor to select the interactions in the targets with only one charge secondary particle after the target with the relative angle to beam particle $\theta > 0.1$ mrad (this system is now in R&D phase (N. Terentiev, private communication)).

6. Possibilities of the search for cryptoexotic strange hyperons $|\, dds s\bar{s}\rangle$ in the experiment E781

In connection with the results of the SPHINX experiment we are considering here the possibility to search for the reactions of diffractive production of cryptoexotic hyperons with additional hidden strangeness $Y_\phi^- = |\, dds s\bar{s}\rangle$ in the 600÷650 GeV Σ^- beam at the Fermilab Tevatron:

$$\Sigma^- + N \to Y_\phi^- + N \tag{17}$$

It is easy to write more than a dozen of possible decay modes for Y_ϕ^- by adding quark-antiquark pairs and combining all the quarks into known particles. A detailed study was made for the following four processes:

$$\begin{array}{lll} Y^- & \to & \Xi^- K_S^0 \\ & & \quad\hookrightarrow \pi^+\pi^- \\ & & \hookrightarrow \Lambda\pi^- \\ & & \quad\hookrightarrow p\pi^- \end{array} \tag{18}$$

$$\begin{array}{lll} Y^- & \to & \Xi(1530)^- K_S^0 \\ & & \quad\hookrightarrow \pi^+\pi^- \\ & & \hookrightarrow \Xi^-\pi^0 \\ & & \quad\hookrightarrow \gamma\gamma \\ & & \quad\hookrightarrow \Lambda\pi^- \\ & & \quad\quad\hookrightarrow p\pi^- \end{array} \tag{19}$$

$$\begin{array}{lll} Y^- & \to & \Sigma^0 K^- K_S^0 \\ & & \quad\hookrightarrow \pi^+\pi^- \\ & & \hookrightarrow \Lambda\gamma \\ & & \quad\hookrightarrow p\pi^- \end{array} \tag{20}$$

$$\begin{array}{lll} Y^- & \to & \Sigma^- K_S^0 K_S^0 \\ & & \quad\hookrightarrow \pi^+\pi^- \\ & & \quad\hookrightarrow \pi^+\pi^- \\ & & \hookrightarrow n\pi^- \end{array} \tag{21}$$

Some other possible decay modes may be found in Table 1.

Table 1. Decay channels and efficiency for detection of diffractively produced cryptoexotic baryon states $Y_\phi^- = | ddss\bar{s}\rangle$ in Σ^- hyperon beam with momentum $P_{\Sigma^-} = 650$ GeV.

n/n	Decay sequence	Mass threshold	$\Pi(\mathrm{br})_i$	Type of trigger	Geometry	Eff. (total)	$(\sigma\cdot\mathrm{BR})_{\mathrm{eff}}$ nb/nucleon	Number of events detected
1	$Y_\phi^- \to \Xi^- K_S^0$, $K_S^0 \to \pi^+\pi^-$; $\Xi^- \to \Lambda\pi^-$, $\Lambda \to p\pi^-$	1819	0.22	1	A	0.047	2.6	5200
					B	0.16	8.7	17300
				2	A	0.040	2.2	4400
		(2250)		(≤ 3)	B	0.13	7.4	14700
				2	A	0.033	1.8	3600
				(≤ 2)	B	0.11	6.0	12000
2	$Y_\phi^- \to \Xi(1530)^- K_S^0$, $K_S^0 \to \pi^+\pi^-$; $\Xi(1530)^- \to \Xi^-\pi^0$, $\Xi^- \to \Lambda\pi^-$, $\Lambda \to p\pi^-$	2033	0.07	1	A	0.023	0.41	820
					B	0.069	1.2	2400
				2	A	0.020	0.35	710
		(2500)		(≤ 3)	B	0.060	1.1	2100
				2	A	0.016	0.28	570
				(≤ 2)	B	0.048	0.85	1700
3	$Y_\phi^- \to \Sigma^0 K^- K_S^0$, $K_S^0 \to \pi^+\pi^-$; $\Sigma^0 \to \Lambda\gamma$, $\Lambda \to p\pi^-$	2185	0.22	1	A	0.15	8.2	16500
					B	0.23	13.0	25600
				2	A	0.11	6.2	12400
		(2750)		(≤ 3)	B	0.18	9.6	19300
				2	A	0.090	4.9	9800
				(≤ 2)	B	0.14	7.7	15400
4	$Y_\phi^- \to \Sigma^- K_S^0 K_S^0$, $K_S^0 \to \pi^+\pi^-$, $K_S^0 \to \pi^+\pi^-$; $\Sigma^- \to n\pi^-$	2193	0.12	1	A	0.23	6.7	13300
					B	0.28	8.0	16000
				2	A	0.18	5.2	10400
		(2750)		(≤ 3)	B	0.22	6.25	12500
				2	A	0.13	3.9	7800
				(≤ 2)	B	0.16	4.7	9300
5	$Y_\phi^- \to \Lambda K^- K_S^0$, $K_S^0 \to \pi^+\pi^-$; $\Lambda \to p\pi^-$	2108	0.22	1	A	0.21	11	22000
					B	0.29	15	30000
6	$Y_\phi^- \to \Omega^- K_S^0 K_S^0$, $K_S^0 \to \pi^+\pi^-$, $K_S^0 \to \pi^+\pi^-$; $\Omega^- \to \Lambda K^-$, $\Lambda \to p\pi^-$	2668	0.079	1	A	0.35	10	20000

n/n	Decay sequence	Mass threshold	$\Pi(\mathrm{br})_i$	Type of trigger	Geometry	Eff. (total)	$(\sigma\cdot\mathrm{BR})_{\mathrm{eff}}$ nb/nucleon	Number of events detected
7	$Y_\phi^- \to \Xi^- K^+ \pi^-$ $\hookrightarrow \Lambda\pi^-$ $\hookrightarrow p\pi^-$	1955	0.64		C	0.10	16	32000
8	$Y_\phi^- \to \Xi^- K^*(892)^0$ $\hookrightarrow K^+\pi^-$ $\hookrightarrow \Lambda\pi^-$ $\hookrightarrow p\pi^-$	2217	0.42	1	C	0.11	11	22000
9	$Y_\phi^- \to \Lambda K^+ K^- \pi^-$ $\hookrightarrow p\pi^-$	2244	0.64	1	C	0.31	50	100000
10	$Y_\phi^- \to \Lambda\phi\pi^-$ $\hookrightarrow K^+K^-$ $\hookrightarrow p\pi^-$	2320	0.32	1	C	0.30	25	50000
11	$Y_\phi^- \to \Sigma^+ K^- K_S^0 \pi^-$ $\hookrightarrow \pi^+\pi^-$ $\hookrightarrow p\pi^0$	2321	0.175	1	C	0.17	7	14000
12	$Y_\phi^- \to \Sigma^- K^+ K^-$ $\hookrightarrow n\pi^-$	2185	1.0	1	B	0.3	75	140000

Notes:

1. In the column *Mass threshold* the values of the mass Y_ϕ^- for which Monte-Carlo calculations were done are presented in parentheses.

2. Trigger conditions:

Type 1. Anticoincidence from Photon 1, anticoincidence from large scintillation counter at the position of hodoscope H2 with size ± 100 cm, ± 50 cm and hole ± 35 cm, ± 10 cm. Multiplicity requirement from hodoscopes H1 and H2 was $3 \leq M_{\mathrm{H1}} \leq M_{\mathrm{H2}} \leq 5$ for geometry B, and the same but without $M_{\mathrm{H1}} = 3$, $M_{\mathrm{H2}} = 3$ for geometry A.

Type 2. Anticoincidence from Photon 1, anticoincidence from small scintillation counter at the position of hodoscope H2 with size ± 60 cm, ± 21 cm and hole ± 35 cm, ± 10 cm. Multiplicity requirements from hodoscopes H1 and H2 are the same as for the type 1 trigger. Five small scintillation counters with size ± 1 cm, ± 1 cm were placed after each group of microstrip detectors. Multiplicity not more than 1 was required in the first two counters, multiplicity ≤ 2 or ≤ 3 was required from the three last counters.

3. For the process number 12 possible trigger is: three particles in interaction counter, hodoscopes H1 and H2, big signal from neutron calorimeter.

4. $\Pi(\mathrm{br})_i$ is the product of branching ratios for visible decays.

5. We suppose that typical $\sigma_{\mathrm{diff}}(Y_\phi^-)\cdot\mathrm{BR}(Y_\phi^- \to YK) \simeq 250$ nb/nucleon (at the same level as for B_ϕ diffractive production in the SPHINX data). We do not use an increasing factor, connected with coherent production of the baryon states on the nuclei with larger value of atomic number A.

6. $(\sigma\cdot\mathrm{BR})_{\mathrm{eff}} = [250\,\mathrm{nb/nucleon}]\cdot[\mathrm{Eff.(total)}]\cdot[\Pi(\mathrm{br})_i]$.

7. The number of events is estimated for $6\cdot 10^{10}$ Σ^- interactions in the targets (16 effective weeks of the run, i.e. $\sim 1/3$ of the total expected run time).

8. In this table we do not include several reduction factors for the efficiency and statistics (accidental losses in anticoincidence counters, efficiency of event reconstruction). We hope that all these factors are not more than a factor of 2 and will be compensated by the real duration of the run.

We suppose to work in parallel with the main program of the E781 experiment connected with the study of charmed and strange-charmed baryons, which imposes certain limitations on any other trigger. So let us consider some basic numbers and requirements. The beam consists of about 50% of Σ^-, and about 50% of π^-. The number of Ξ^- in the beam is not known with any good accuracy, but it is of an order of 1%. The beam intensity is $2{\cdot}10^6\,s^{-1}$. Data acquisition is supposed to accept events from the charm trigger at the rate of $10^4\,s^{-1}$. The dead time introduced by all other triggers should not exceed 10% of the dead time caused by the charm trigger. As the events corresponding to other triggers are expected to be more simple and cause less dead time than charm trigger events, it is probable that admissible quota of additional triggers events is a bit more than 10%. Triggers are proposed for the study of Primakoff effect physics and $\Sigma^- e$ scattering. That means that each individual trigger should be of an order of few percent of charm trigger. Furthermore, overall trigger scheme is multilayered, so it is necessary to have an acceptable rate at each trigger level.

7. Trigger, efficiency and background study

Calculations of efficiency of processes (18)–(21) and trigger background were made using the GE781 program. Unfortunately, there was no stable version of it during our stay there. The best way to describe the version is to say that it was taken from the directory
/usr/products/IRIX/e781mc/devel/src/car
on November 17, 1994 at 12:10, and some minor corrections and changes were introduced. Model of E781 facility contained the following detectors:
BSCI — beam scintillation counters,
BSSD — beam silicon strip detectors,
DDCH — downstream drift chambers,
DPWC — downstream proportional wire chambers,
HODO — hodoscopes,
LASD — large angle silicon detectors,
LPWC — lambda proportional wire chambers,
LSCI — lambda scintillators,
RICH — ring-image Cherenkov counter,
PHOT — electromagnetic calorimeters,
TRAD — transition radiation detector,
TRSD — trigger silicon detectors,
UPWC — upstream proportional wire chambers,
VEEC — vee chambers,
VSSD — vertex silicon strip detectors.

There were no interaction counters in the program. Each of them will have the width of about 1.5 mm, which corresponds to 0.37% of interaction length. As there is about 3.7% of interaction length between the target and hodoscope H1, the absence of interaction counters does not influence the results significantly.

There was no digitization of hodoscopes in the program, and the structure of them has not been settled yet. Digitizations in hodoscopes were determined for the following structure

	H1		H2	
	Counters	Size, cm	Counters	Size, cm
Center			4	4.0
	4	2.5	6	2.5
	4	2.0	6	2.0
	5	1.5	8	1.5
	3	1.0	3	1.0
	6	0.5	8	0.5
	3	1.0	3	1.0
	5	1.5	8	1.5
	4	2.0	6	2.0
	4	2.5	6	2.5
			4	4.0
Total:	38	60.0	62	120.0

Vertical sizes of the hodoscopes were 30 and 42 cm, correspondingly. The results do not depend significantly upon reasonable modifications of the hodoscopes structure. The efficiency of hodoscopes was taken to be 100%. An effect of one charged particle hitting adjacent counters and thus producing two digitizations was not taken into account.

There was no digitization of the Photon 1 detector in the program. When including it into anticoincidence it was required that no particles should hit it. Certainly, as a matter of fact some energy threshold will be set. If that threshold may be set to a value of an order of 1 GeV, then an increase in the trigger background will be no more than 1.5÷2.0 (it was obtained in some preliminary study).

Default GEANT processes and cuts were used for trigger background calculations. When calculating the efficiency only DCAY, LOSS, MULS (particle decay, ionization loss, multiple scattering) processes were allowed. Decay branching ratios for the particles of interest were set to be 100%. Lifetime of charged pions and kaons was set to be a big number, so no decays of these particles occured. The efficiency determined in such a way is sometimes referred to as the geometrical efficiency.

There is a serious problem concerning simulation of the very first interaction of beam particles. Several methods of playing the interaction were tried: default GEANT, minimum bias events Σ^-Al generated by FRITIOF-7.02a (file **run04.dat**), $\Sigma^- n$ events generated by PYTHIA-5.702. Default GEANT interactions and FRITIOF events give compatible trigger levels, while for PYTHIA events it is substantially higher (factor about 5). From the physical point of view the main difference between PYTHIA and FRITIOF simulations is that diffractive production processes are not used in FRITIOF, while PYTHIA is not able to simulate interactions on nucleus. The best approximation at the moment is, probably, events in the file **pi_c_600a.dat**. These events, as it was pointed by J. Russ,

are in a reasonable accordance with experimental data. They give trigger level somewhere in-between that of PYTHIA and FRITIOF. All figures and numbers presented below are for that kind of primary interaction if not explicitly specified otherwise.

7.1. Characteristics of processes of interest

In order to construct a trigger we need to know the properties our events possess. For processes (18)–(21) the main characteristics are:

1. One charged particle after the interaction.
2. Five charged particles after all weak decays of K_S^0 mesons and hyperons have taken place.
3. Usually all five charged particles have high momentum (sufficient to pass through M1 and M2).
4. Charged particles have narrow distribution in XY-plane at positions of hodoscopes H1 and H2.
5. Charged particles and gammas (if present in the event) rarely hit Photon 1 detector.
6. Charged particles and gammas (if present in the event) often hit Photons 2 and 3.

As the processes under consideration are exclusive, all these features are almost evident, so we do not provide figures with the corresponding distributions. However, we make exception for the distribution of the particle energies, which are presented in Fig. 8 for process (19) for $M(Y_\phi^-) = 2.5\,\mathrm{GeV}$.

To organize trigger for these processes it seems natural to use the requirement of multiplicity to be 1 in the interaction counters and some multiplicity increase in hodoscopes H1 and H2. Tables of hodoscopes multiplicities are presented in Fig. 9. We would like to use multiplicity requirement shown by bold lines on that figure.

7.2. Trigger and background

There are few sources of the trigger background: interactions in the matter of the setup, decays of beam Ξ^- particles, muons originating from the target of hyperon channel.

We suppose to use the beam TRD to select Σ^- beam particles. If not explicitly specified, in any numbers given below factor 1/2 was introduced for Σ^- selection. Background events in which the first interaction has taken place before or in the target will be suppressed by multiplicity 1 requirement in interaction counters. Events, in which the first interaction has taken place after the hodoscope H1, will be suppressed by the multiplicity requirement from H1. Events with the first interaction after the target but before hodoscope H1 are the most likely source of background. There is $\simeq 3.7\%$ of interaction length between the last target and hodoscope H1, which corresponds to the trigger rate $3.7{\cdot}10^4\,\mathrm{s}^{-1}$. Distribution of the Z-coordinate of the primary interaction is presented in Fig. 10. It is clearly seen that the main source of interactions is microstrip detectors. After the multiplicity requirement from hodoscopes H1 and H2 (as shown in Fig. 9) the remaining trigger rate is $1.0{\cdot}10^4\,\mathrm{s}^{-1}$. Apparently a lot of particles do not reach hodoscopes.

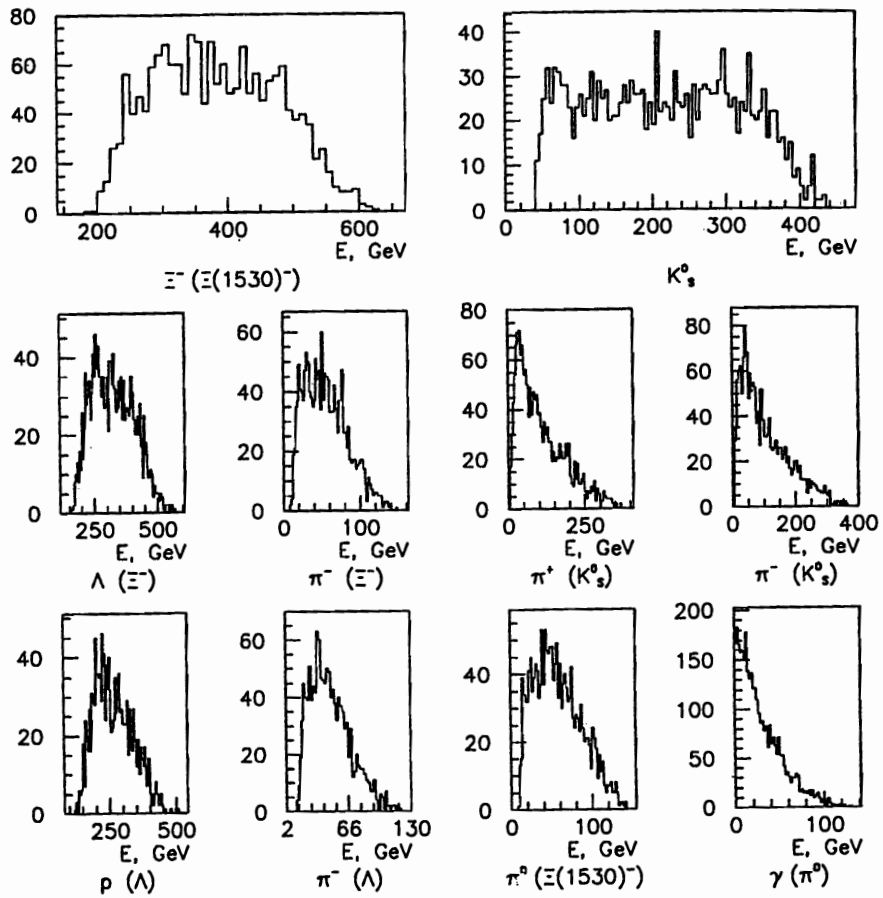

Fig. 8. Particles energy in the process (19) $Y_\phi^- \to \Xi(1530)^- K_S^0$ for $M(Y_\phi^-) = 2.5$ GeV.

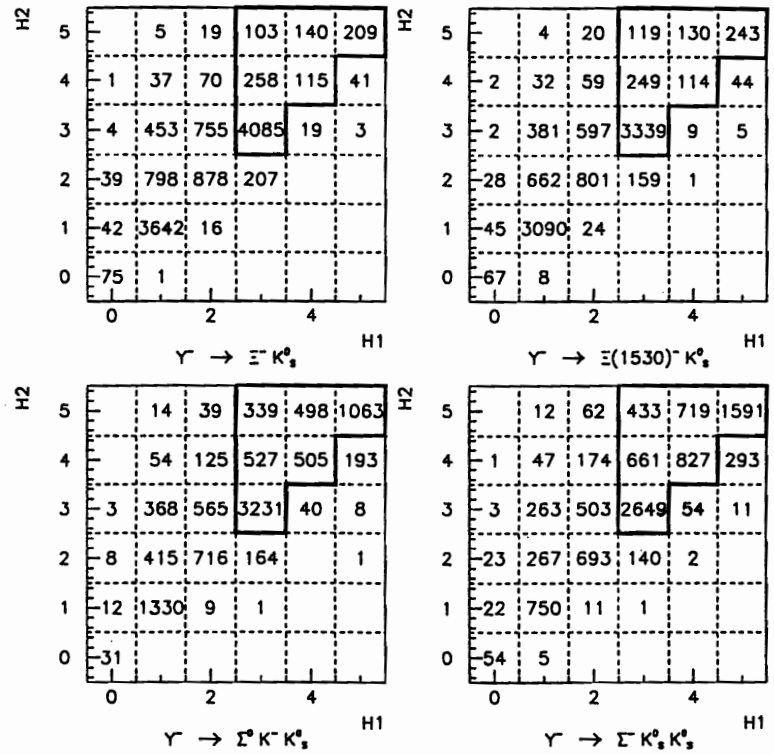

Fig. 9. Multiplicity in hodoscopes H1 and H2 for processes (18)–(21).

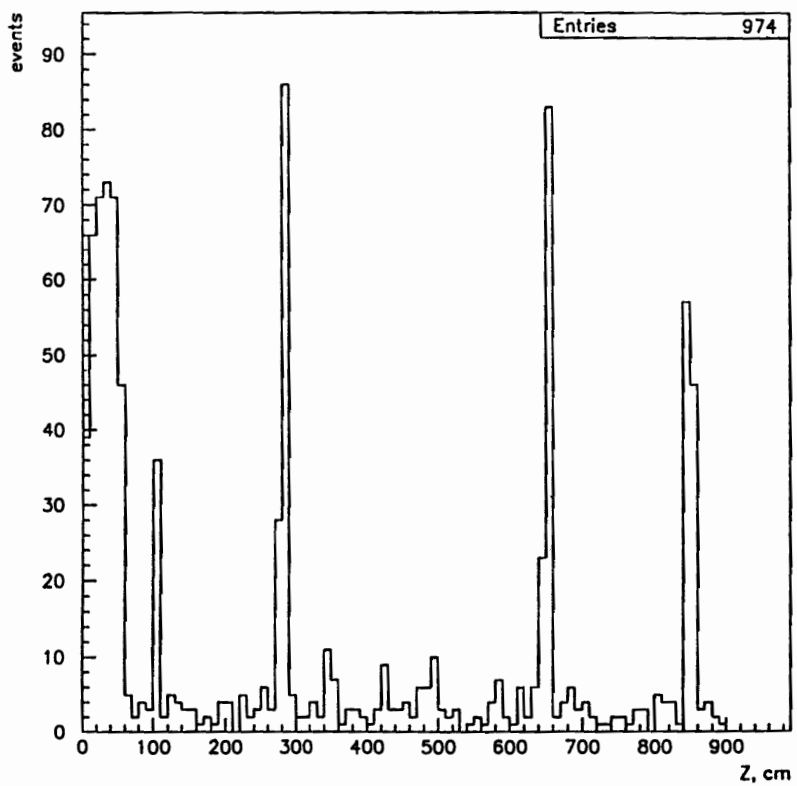

Fig. 10. The Z-coordinate distribution of the first interaction of beam particle between the interaction counters and hodoscope H1.

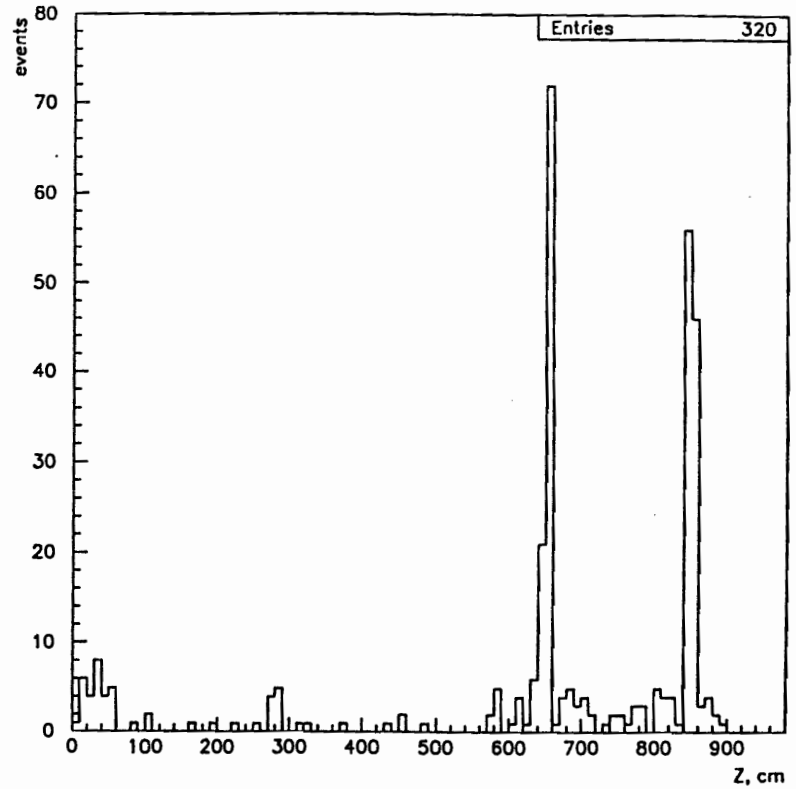

Fig. 11. The Z-coordinate distribution of the first interaction of beam particle between the interaction counters and hodoscope H1 after requirement of anticoincidence from Photon 1.

One of the possibilities to suppress background is to use anticoincidences. It seems natural to kill the background from the events in which interaction has taken place before Photon 1 detector by including it in anticoincidence. Distribution of the Z-coordinate of the primary interaction events remaining after this procedure is presented in Fig. 11. It is seen that the background from those events is suppressed significantly. But still the remaining background rate is $2.2 \cdot 10^3\,\mathrm{s}^{-1}$. If we look now at the distribution of charged particles in the XY-plane at the position of hodoscope H2 (Fig. 12), we see that it is very wide. At the same time charged particles from processes (18)–(21) are concentrated mainly in the region ± 35 cm, ± 10 cm. If we use an anticoincodence counter with a hole of that size and external dimensions ± 100 cm, ± 50 cm, the trigger rate will drop to $3.8 \cdot 10^2\,\mathrm{s}^{-1}$, which constitutes 3.8% of the nominal charm trigger. We will refer to the described set of trigger conditions as Trigger 1.

One more factor that may influence the trigger is muon flux from the hyperon target. It is not well known yet. According to estimates of P. Cooper, muon rate can be up to $10\,\mathrm{MHz/m^2}$ at the position of the hodoscope H2. If we use anticoincidence counter with specified dimensions, we will loose $\sim$ 37% of the events. Simulteneously we loose the same percent of background events. Besides muon flux will lead to multiplicity increase in hodoscopes H1 and H2, so we pick up some events with low original multiplicity, and lose some events with high original multiplicity. These contributions cancel each other to some extent. As Photon 1 energy threshold will (almost for sure) be more than 1 MIP, muons influence on the calorimeter is rather small.

We conclude that it is possible to work with Trigger 1. However, due to uncertainties in the muon background and some technical problems of arranging large scintillation counter around the hodoscope H2, we considered another possibility to kill the background. Let us designate it as Trigger 2.

As it is seen from Fig. 10, the main source of interactions is microstrip detectors. As it is not possible to obtain information from these detectors at hardware trigger level, we can use small thin scintillation counters, placed after each group of microstrip detectors (vertex, trigger, LASD after M1, before M2, after M2). We are going to set the upper limit on the number of charged particles in each of them, so the amplitude analysis must be performed. Multiplicities of charged particles in the plane of the last silicon strip detector in each group for three different dimensions (with the size that of the last detector, $3 \times 3\,\mathrm{cm}^2$, $2 \times 2\,\mathrm{cm}^2$) for process (18) with the equal number of events with mass 2.0 GeV and 2.5 GeV are presented in Fig. 13.

As it follows from Fig. 13, we can set upper limit 1 on the number of charged particles in the counters of both sizes placed after vertex and trigger silicon detectors without any significant loss in effciency. We would like also to set upper limit 2 or 3 for other three counters. But upper limit 2 for the counters with the size greater than ± 1 cm, ± 1 cm leads to substantial loss in efficiency for the near-threshold mass region of the produced system.

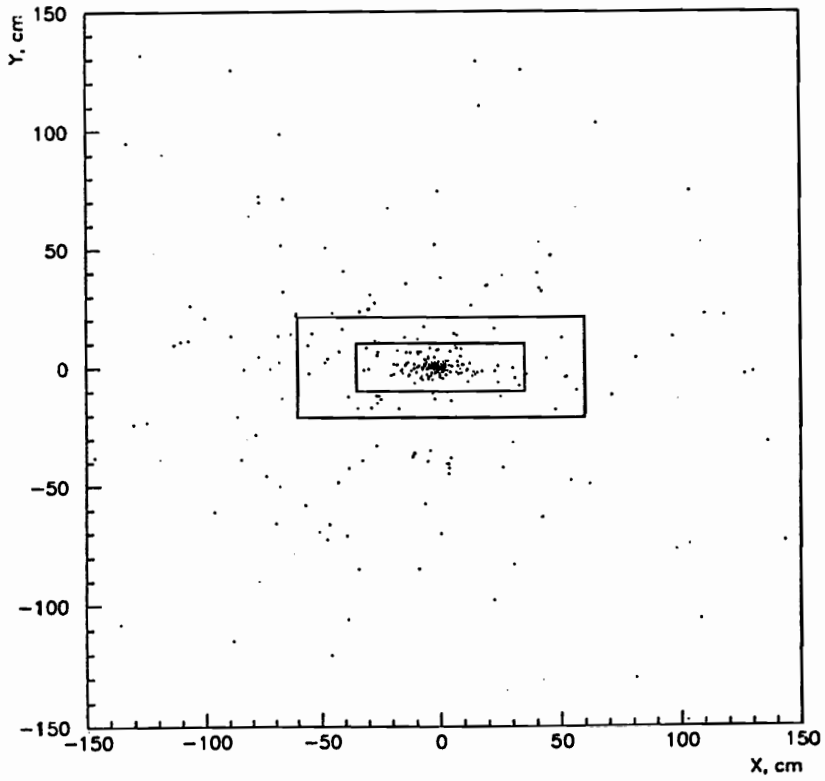

Fig. 12. The distribution of charged particles at the hodoscope H2 position after the requirement of multiplicity combination and anticoincidence from Photon 1.

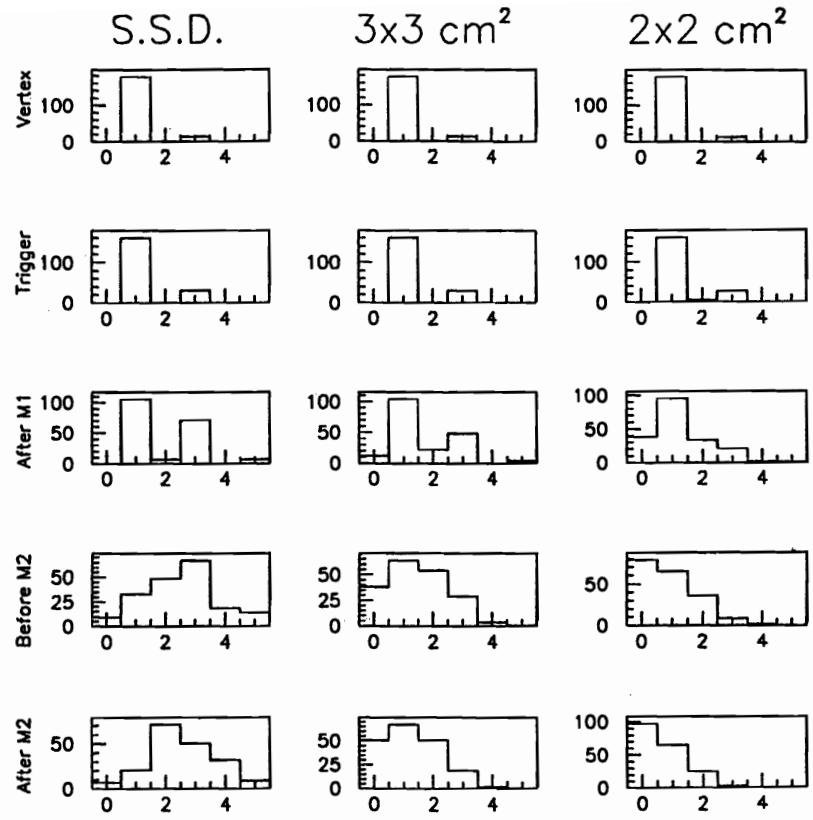

Fig. 13. Charged particles multiplicity in silicon strip detectors for process (18) after the multiplicity requirement from the hodoscopes H1 and H2. The equal number of events with mass 2.0 GeV and 2.5 GeV were generated.

Thus we chose size of counters to be ±1 cm, ±1 cm, and calculations, presented below, refer to that option. The usage of these counters allows one to lessen the dimensions of large anticoincidence counter to the size of hodoscope H2 (±60 cm, ±21 cm) with the same hole (±35 cm, ±10 cm). Thus constructed Trigger 2 will have rate $5.6 \cdot 10^2\,s^{-1}$ for upper limit 3 in the last three counters, which constitutes 5.6% of the nominal charm trigger. It can be reduced further by setting upper limit 2 in some counters.

Detailed information on the background levels for different types of triggers is presented in Table 2.

Table 2. Trigger rates for different trigger options and primary interactions.

Trigger	Geometry	FILE pi_c_600a	GEANT π^- beam	FRITIOF $\Sigma^- Al$	PYTHIA $\Sigma^- n$
Trigger 1	A	320	140	160	360
	B	760	300	160	1060
Trigger 2 (≤ 3)	A	160	160	200	220
	B	560	300	200	600
Trigger 2 (≤ 2)	A	120	100	160	160
	B	280	160	160	360

Possibilities to work with multiplicity combination $M_{H1} = 3$, $M_{H2} = 3$ in the hodoscopes may be limited by another source of background, connected with decay of the beam Ξ^- particles

$$\begin{array}{lll} \Xi^- & \rightarrow & \Lambda\pi^- \\ & & \hookrightarrow p\pi^- . \end{array} \tag{22}$$

We suppose that those events, where Λ was produced and has decayed before the interaction counter, will be eliminated by the requirement of multiplicity 1 in the interaction counters. For those events in which Λ has decayed after the interaction counters table of hodoscope multiplicities is presented in Fig. 14 (for 10000 Ξ^-). Though we do not know exactly how many Ξ^- particles will be in the beam, it is clear that it is an essential source of background ($5.4 \cdot 10^2\,s^{-1}$ per 1% of Ξ^- in the beam). What can we do with this sort of background? There are three possibilities:

1. Not to use multiplicity requirement $M_{H_1} = 3$, $M_{H_2} = 3$ in the trigger. As it follows from the hodoscope multiplicity tables in Fig. 9, this requirement is significant for processes (18) and (19), in which double weak decay chain ($\Xi^- \rightarrow \Lambda\pi^-$, $\Lambda \rightarrow p\pi^-$) is present, and less essential for processes (20) and (21) without such double weak decay sequence.
2. To prescale the trigger with that multiplicity combination.

3. To require the increase in charged particles multiplicity in some place downstream with respect to hodoscope H2. Rather reasonable way to do this is to use some additional hodoscope (let us call it H3), placed right after the RICH. It would provide more than 10 m additional decay base, while charged pions from the K_S^0 decay are distributed not very widely.

Each of the last two methods has weak and strong points. Using prescaling, we loose some events, but the path where Λ decays may be registered is longer. Using multiplicity increase, we have guarantee that Λ decay has really taken place.

7.3. Efficiency calculations and estimations

There is a lot of possible decay modes of cryptoexotic pentaquark baryons $|\, ddss\bar{s}\rangle$. Those with just one charged particle after the interaction and five charged particles after all weak decays we will call processes of $1 \rightarrow 5$ type. We present results for the worst and the best (but reasonable) cases. In the worst case all weak decays must occur before hodoscope H2 (decay length 1216 cm), and at least three charged particles must pass through hodoscope H1 (decay length 905 cm). We will refer to that case as "geometry A". In the best case all weak decays must occur before the second block of vee drift chambers VEEB, which corresponds to 3350 cm decay length. If a new hodoscope H3 is placed after the RICH, thus reducing decay path to 2750 cm, it will lead to less than 15% reduction in efficiency. We will not distinguish between these two options and mark them as "geometry B".

There are also decay modes with three charged particles after the interaction and five after all weak decays. We will call them processes of $3 \rightarrow 5$ type. We require five charged particles in the hodoscope H2, and will refer to this case as "geometry C".

For processes (18)–(21) efficiency for the worst case of Trigger 1 (geometry A) is presented in Fig. 15 as a function of mass. It was required that photons (if present) hit either Photon 2 or 3, and neutron (if present) hit Photon 3. Efficiencies of the same processes for Trigger 2 with multiplicity upper limits 3 and 2 in the last three scintillation counters after microstrip detectors are presented in Fig. 16 and 17 respectively.

When estimating total efficiency and the number of events registered some additional correction factors were applied: 0.7 for the registration of single photon, 0.5 for the registration of π^0 meson, 0.8 for the registration of neutron. For processes other than (18)–(21) total efficiency and expected statistics were estimated with the account of average decay probabilities and setup efficiency. Results of these approximate evaluations for processes (18)–(21) are in good agreement with more detailed Monte-Carlo studies, so we consider them to be quite reliable for other processes as well. All efficiency and statistics evaluations are summarized in Table 1, more information is in the notes to this table.

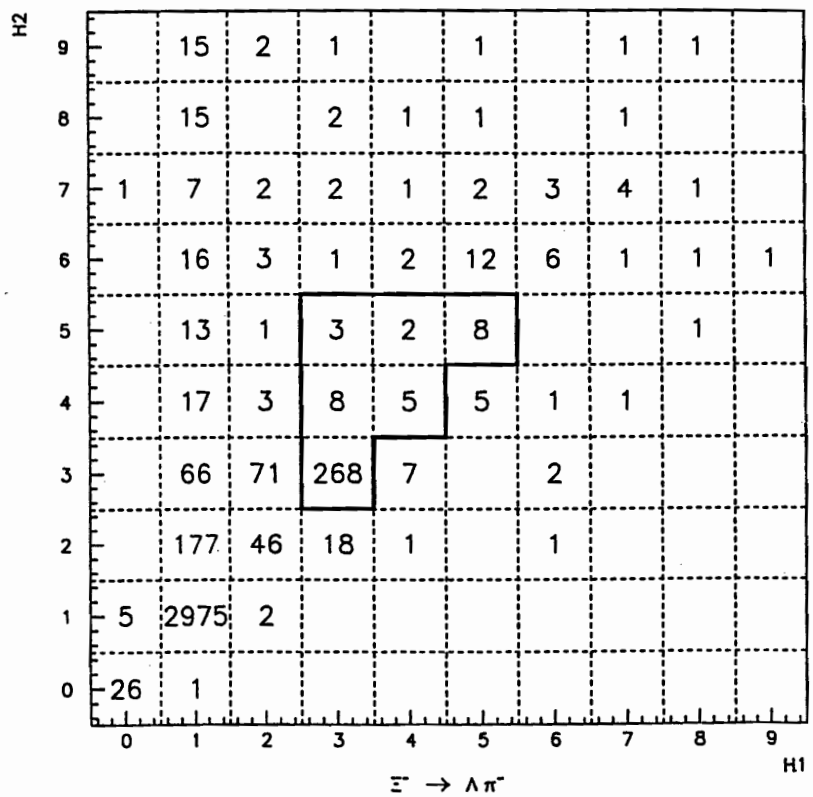

Fig. 14. Multiplicity in hodoscopes H1 and H2 for process (22) for 10 000 beam Ξ^-.

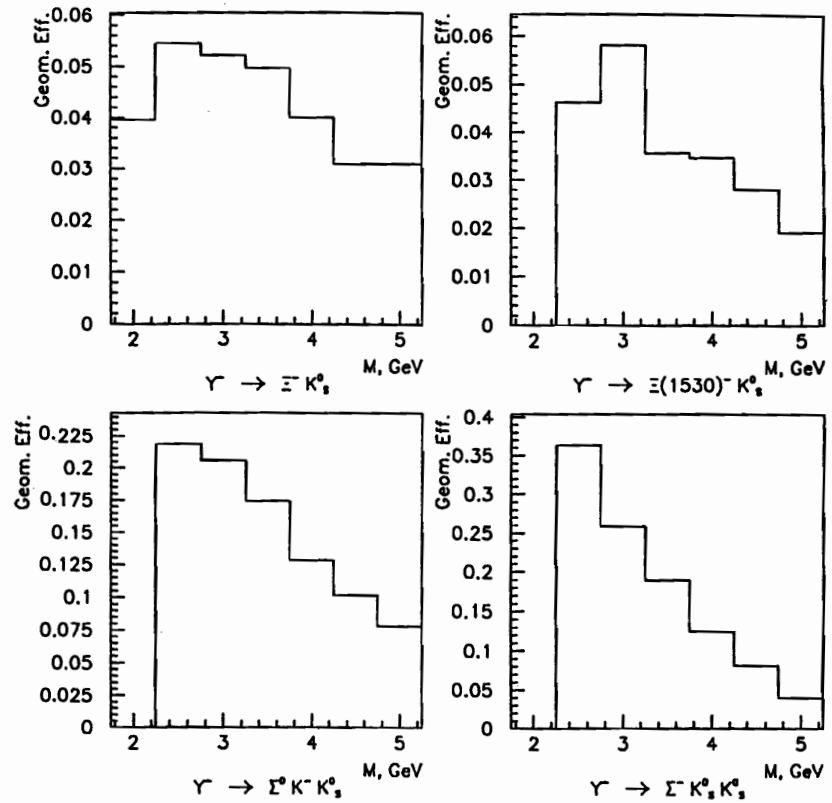

Fig. 15. Geometrical efficiency for processes (18)–(21) for geometry A (the worst case) for Trigger 1.

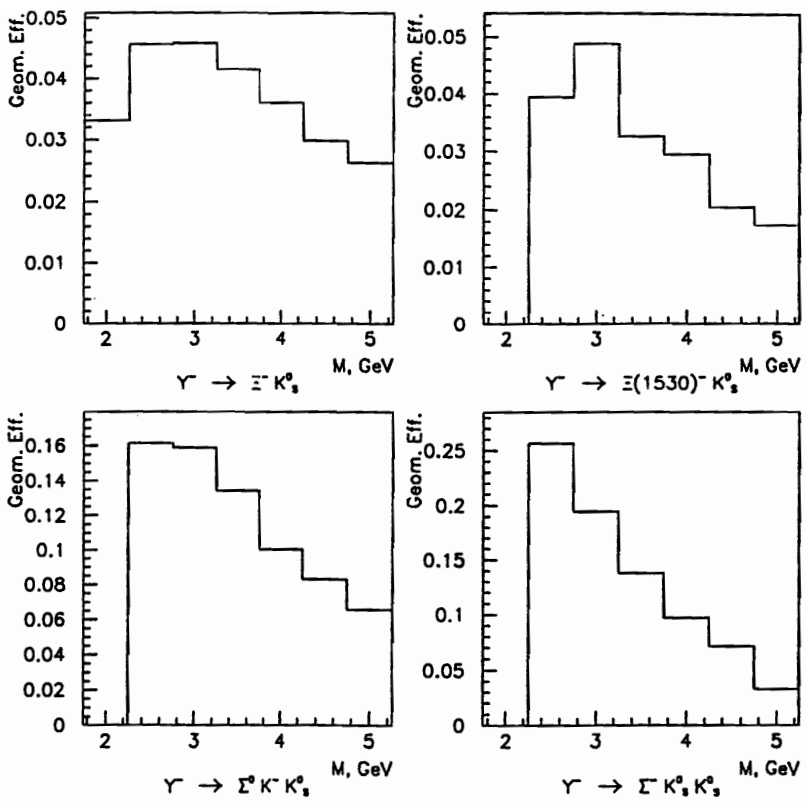

Fig. 16. Geometrical efficiency for processes (18)–(21) for geometry A (the worst case) for Trigger 2 with upper limit 3 in the last three counters after microstrips.

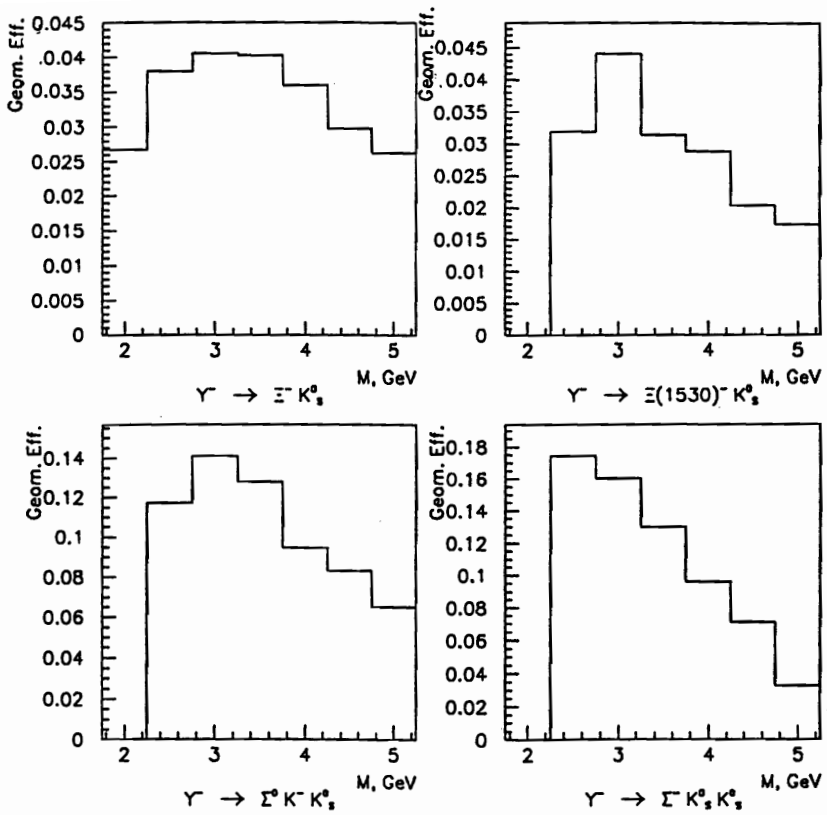

Fig. 17. Geometrical efficiency for processes (18)–(21) for geometry A (the worst case) for Trigger 2 with upper limit 2 in the last three counters after microstrips.

8. Constructing the trigger

While the issue with fast hardware trigger for Primakoff polarizability measurements of π^- and Σ^- is not clear, it seems approapriate to make few comments concerning possibility of using it in our trigger scheme. If that trigger is capable to register that interaction occured in the target, then it can be used for our trigger and will reduce the background significantly. If it registers the absence of a beam particle in some point downstream, it suppresses only those interactions that would occur after that point. Finally, if that point is at position of hodoscope H1 or further, it is of no use, as we require at least three particles in H1.

The trigger with the multiplicity requirement $M_{\mathrm{H1}} = 3$, $M_{\mathrm{H2}} = 3$ may be used (appropriatly prescaled) for triggering the Ξ^- decays (22), where Λ has decayed before H1 (which may be useful for monitoring the apparatus), and also for some processes of the Primakoff production, e.g.:

$$\begin{array}{lcl} \Sigma^- + (Z,A) & \rightarrow & \Sigma(1385)^- + (Z,A) \\ & & \quad \hookrightarrow \Lambda\pi^- \\ & & \qquad \hookrightarrow p\pi^- \end{array} \tag{23}$$

More information about the Primakoff production of excited hyperons may be found, for example, in [32].

8.1. Trigger devices

Here we summarize all the devices needed for our trigger and what we are going to require from them:

1. **Beam TDR:** beam particle to be Σ^-.
2. **Interaction counters:** multiplicity 1 in this device.
3. **Hodoscope H1:** multiplicity 3÷5 at $L0$ level.
4. **Hodoscopes H1, H2:** multiplicity combination as shown in Fig. 9.
5. **Hodoscope H2:** some margin counters to be included in anticoincidence.
6. **Anticoincidence counter:** it is obvious.
7. **Photon 1:** anticoincidence from it.
8. **Scintillation counters after microstrips:** multiplicity of charged particles in any counter not to exceed some upper limit. We need to be able to set that limit to any value between 1÷3.
9. *Hodoscope H3:* some multiplicity signal (presumably 4÷5). We need a possibility to use it with multiplicities in hodoscopes H1 and H2 $M_{\mathrm{H1}} = 3$, $M_{\mathrm{H2}} = 3$ alone as well as with all other multiplicity combinations. It would be desirable to have as much flexibility of using H3 in the trigger as possible.

8.2. Matching the trigger levels

8.2.1. Level 0

As processes (18)–(21) are characterized by only one charged particle just after the interaction, they are not distinguishable from the beam by any fast device in the interaction region. In order to discriminate against the beam it is necessary to use some fast device rather far downstream to provide sufficient decay base for K_S^0 and Λ. There are only two such devices in the SELEX facility — hodoscopes H1 and H2. It is possible and does not seem to be difficult to include multiplicity signal from hodoscope H1 in the trigger at $L0$ level without hampering with charm trigger (A. Kulyavtsev, private communication). The interaction counter will also be included in the trigger at $L0$ level, and it helps to discriminate against interaction before and in the target with multiplicity of charged particles more than one.

8.2.2. Levels 1 and 2

Trigger signals from other detectors (beam TRD, combination of multiplicities in H1 and H2 hodoscopes, Photon 1, anticoincidence counters, maybe something else) participate at $L1$ or $L2$ levels. It is not of crucial importance at what trigger level a signal from any given detector is incorporated.

8.2.3. Level 3

Processes we are looking for are relatevely simple, and there is no doubt that many ways exist to select events with a computer filter. But one of them deserves to be mentioned right now: matching the beam track with hits (tracks) in vertex silicon strip detectors (in fact, it is implementation of the Primakoff trigger in the computer filter). The simplest way to do this is to require that there be no beam track continuation in the vertex silicon strips. That will guarantee that something has happend with beam particle before or in the target, and it is either the interaction of the type we are looking for, or decay (e.g. $\Xi^- \to \Lambda\pi^-$). Such a procedure may be called "killing the beam", as it does not guarantee interaction. If it were possible to find a Z-coordinate of the kink (no great accuracy needed), then it would be an effective way to discriminate against decays outside the target region.

8.3. Controlling the trigger rate

When any experiment is under way, it is very important to be able to control trigger rate. There are the following ways to control our trigger:

1. to prescale the trigger. Due to Ξ^- decays (22) and a possibility to use hodoscope multiplicity combination $M_{H1} = 3$, $M_{H2} = 3$ for some other triggers (see section 8), it is necessary to be able to prescale that multiplicity combination independently of all others.

2. to adjust energy threshold in Photon 1. In fact, we would like to set it as low as possible, but too low threshold would lead to random anticoincidence signals from noise, muons, etc.
3. to select counters in hodoscope H2 which are included in anticoincidence (but counters in the central part will never be used for that purpose in our trigger). Thus we are able to lower trigger rate at a price of efficiency for high mass region.
4. to be able to control multiplicity combinations of hodoscopes H1 and H2 which participate in the trigger. That adds flexibility to the trigger.
5. to adjust the multiplicity requirements in small scintillation counters placed after each group of microstrip detectors.

Acknowledgements.
This work was done in the end of 1994, when the authors were at Fermilab and had an opportunity to participate in E781 collaborations meetings and discussions. It is a pleasure for us to express our gratitude to P. Cooper, M. Kubantsev, A. Kulyavtsev, N. Kuropatkin, J. Russ and other members of the collaboration for stimulating discussions. We are also indebted to the Fermilab Directorate for hospitality and the Russian Ministry of Science for financial support.

References

[1] Chung S.-U. – Preprint BNL 40599, Upton, 1987;
Chung S.-U.//Nucl. Phys., 1988, v.473A, p.511;
Chung S.-U.//Z. Phys., 1990, v.46C, p.111.

[2] Landsberg L.G.//UFN, 1990, v.160, p.1;
Landsberg L.G.//Surveys in High Energy Phys., 1992, v.6, p.257;
Landsberg L.G.//Yad. Fiz., 1994, v.57, p.47.

[3] Peters K. – Proc. of the Second Biennial Conf. on Low Energy Antiproton Phys. (LEAP–92). Courmayeur, Aosta Valley, Italy, September 14–19, 1992, Ed. C. Guaraldo et al., p.93.

[4] Close F.E. – Preprint RAL–87–072, Chilton, 1987.

[5] Landsberg L.G.//UFN, 1994, v.164, p.1129.

[6] Hirose T. et al.//Nuov. Cim., 1979, v.50A, p.120;
Fucunage C. et al.//Nuov. Cim., 1980, v.58A, p.199.

[7] Amirzadeh J. et al.//Phys. Lett., 1979, v.89B, p.125.

[8] Aleev A.N. et al.//Z. Phys., 1984, v.26C, p.205.

[9] Karnakov V.M. et al.//Phys. Lett., 1992, v.132B, p.148.

[10] Vavilov D.V. et al.//Yad. Fiz., 1994, v.57, p.241.

[11] Balatz M.Ya. et al.//Z. Phys., 1994, v.61C, p.220.

[12] Balatz M.Ya. et al.//Z. Phys., 1994, v.61C, p.399.

[13] Vavilov D.V. et al.//Yad. Fiz., 1994, v.57, p.253.

[14] Landsberg L.G. – Preprint IHEP 93–100, Protvino, 1993;
Nuov. Cim. (in press).

[15] Vavilov D.V. et al.//Yad. Fiz., 1994, v.57, p.129.

[16] Kurshetsov V.F., Landsberg L.G.//Yad. Fiz., 1994, v.57, p.2030.

[17] Golovkin S.V. et al. – Preprint IHEP 94–78, Protvino, 1994;
Yad. Fiz. (in press).

[18] Chan Hong-Mo, Högaasen H.//Phys. Lett., 1977, v.72B, p.121;
Chan Hong-Mo et al.//Phys. Lett., 1978, v.76B, p.634.

[19] Högaasen H., Sorba P.//Nucl. Phys., 1978, v.145B, p.119;
Invited Talk on Conf. on Hadron Interactions at High Energy, Marseiler, June, 1978.

[20] De Crombrugghe et al.//Nucl. Phys., 1979, v.156B, p.347.

[21] Pietrzuk B. – Preprint CERN–EP/80–116, Geneva, 1980; Talk given at the Fifth European Symposium on Nucleon Interactions, Bressanone, June 23-28, 1980.

[22] Montanet L. et al. (PDG)//Phys. Rev., 1994, v.50, p.1173.

[23] Moinester M.A. et al.//Phys. Rev., 1992, v.46C, p.1082;
Landsberg L.G. et al. – Preprint IHEP 94–19, Protvino, 1994.

[24] Bellini G. et al.//Nuov. Cim., 1984, v.79A, p.282.

[25] Alde D. et al.//Phys. Lett., 1986, v.182B, p.105.

[26] Alde D. et al.//Yad. Fiz., 1991, v.54, p.745;
Alde D. et al.//Phys. Lett., 1992, v.284B, p.457.

[27] Alde D. et al.//Phys. Lett., 1989, v.216B, p.447.

[28] Alde D. et al.//Yad. Fiz., 1991, v.54, p.751;
Alde D. et al.//Phys. Lett., 1992, v.276B, p.375.

[29] Gershtein S.S. – Proc. of the Third Intern. Conf. on Hadron Spectroscopy ("Hadron-89"), Ajaccio, Corsica, September 23-27, 1989, Ed. F. Binon et al., Paris, 1989, p.175.

[30] Edelstein R. et al. – Fermilab Proposal E781 (1987) (revised July, 1993).

[31] Workshop of E781 Collaboration ("E781 Physics Days"), 18–19 August, 1993, Internal Note H-639.

[32] Landsberg L.G. – Proceedings of Workshop UNK–600, IHEP, Protvino, 23-24 of November, 1993. Protvino, 1994, p.27.

Received February 14, 1995

Л.Г.Ландсберг, В.В.Молчанов
О возможных поисках криптоэкзотических странных барионов с дополнительной скрытой странностью в экспериментах на гиперонных пучках высоких энергий.

Оригинал-макет подготовлен с помощью системы LaTeX.
Редактор Е.Н.Горина. Технический редактор Н.В.Орлова.

Подписано к печати 16.02.1995 г. Формат 60 × 84/8. Офсетная печать.
Печ.л. 3,87. Уч.-изд.л. 2,97. Тираж 240. Заказ 290. Индекс 3649.
ЛР №020498 06.04.1992 г.

ГНЦ РФ Институт физики высоких энергий
142284, Протвино Московской обл.

Индекс 3649

П Р Е П Р И Н Т 95-25, И Ф В Э, 1995